Hamel, E., & Lin, C. M. (1981b) *Proc. Natl. Acad. Sci. U.S.A. 78*, 3368–3372.

Hamel, E., del Campo, A. A., Lowe, M. C., & Lin, C. M. (1981) *J. Biol. Chem. 256*, 11887–11894.

Hamel, E., del Campo, A. A., Lowe, M. C., Waxman, P. G., & Lin, C. M. (1982) *Biochemistry 21*, 503–509.

Hamel, E., del Campo, A. A., Lustbader, J., & Lin, C. M. (1983) *Biochemistry 22*, 1271–1279.

Jameson, L., & Caplow, M. (1980) *J. Biol. Chem. 255*, 2284–2292.

Karr, T. L., Podrasky, A. E., & Purich, D. L. (1979) *Proc. Natl. Acad. Sci. U.S.A. 76*, 5475–5479.

Kobayashi, T. (1974) *J. Biochem. (Tokyo) 76*, 201–204.

Kobayashi, T. (1975) *J. Biochem. (Tokyo) 77*, 1193–1197.

Lustbader, J., & Hamel, E. (1982) *Biochim. Biophys. Acta 719*, 215–222.

MacNeal, R. K., & Purich, D. L. (1978) *J. Biol. Chem. 253*, 4683–4687.

Margolis, R. L. (1981) *Proc. Natl. Acad. Sci. U.S.A. 78*, 1586–1590.

Penningroth, S. M., & Kirschner, M. W. (1977) *J. Mol. Biol. 115*, 643–673.

Sandoval, I. V., Jameson, J. L., Niedel, J., MacDonald, E., & Cuatrecasas, P. (1978) *Proc. Natl. Acad. Sci. U.S.A. 75*, 3178–3182.

Schiff, P. B., & Horwitz, S. B. (1981) *Biochemistry 20*, 3247–3252.

Schlesinger, M. J., & Coon, M. J. (1960) *Biochim. Biophys. Acta 41*, 30–36.

Sutherland, J. W. H. (1976) *Biochem. Biophys. Res. Commun. 72*, 933–938.

Terry, B. J., & Purich, D. L. (1980) *J. Biol. Chem. 255*, 10532–10536.

Weisenberg, R. C., & Deery, W. J. (1976) *Nature (London) 263*, 792–793.

Weisenberg, R. C., Borisy, G. G., & Taylor, E. W. (1968) *Biochemistry 7*, 4466–4479.

Weisenberg, R. C., Deery, W. J., & Dickinson, P. J. (1976) *Biochemistry 15*, 4248–4254.

Zabrecky, J. R., & Cole, R. D. (1982) *Nature (London) 296*, 775–776.

Zackroff, R. V., Weisenberg, R. C., & Deery, W. J. (1980) *J. Mol. Biol. 139*, 641–659.

Solution Conformation of Asparagine-Linked Oligosaccharides: α(1–2)-, α(1–3)-, β(1–2)-, and β(1–4)-Linked Units[†]

Jean-Robert Brisson and Jeremy P. Carver*

ABSTRACT: The solution conformation is presented for representatives of each of the major classes of asparaginyl oligosaccharides. In this report the conformation of α(1–3)-, α(1–2)-, β(1–2)-, and β(1–4)-linked units is described. The conformational properties of these glycopeptides were determined by high-resolution ^{1}H nuclear magnetic resonance in conjunction with potential energy calculations. The NMR parameters that were used in this analysis were chemical shi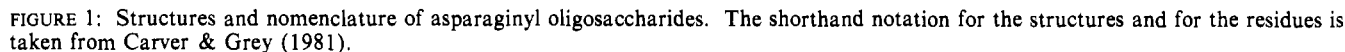fts and nuclear Overhauser enhancements. Potential energy calculations were used to evaluate the preferred conformers available for the different linkages in glycopeptides and to draw conclusions about the behavior in solution of these molecules. It was found that the linkage conformation of the Manα1–3 residues was not affected by substitution either at the 2-position by αMan or βGlcNAc or at the 4-position by βGlcNAc or by the presence of a bisecting GlcNAc on the adjacent βMan residue.

Asparagine-linked oligosaccharides are structurally similar in that most contain the same mannotriose unit; however, they differ in the pattern of substitution of this core and can be classified according to these different patterns (Carver & Grey, 1981). This variability in structure makes them ideally suited for their postulated role as specific recognition signals on the cell surface (Hughes & Sharon, 1978). Although the behavior of these glycopeptides toward lectins (Goldstein & Hayes, 1978), glycosidases, and transferases has been well documented in recent years (Schachter & Roseman, 1980), most of these interactions have only been characterized in terms of the oligosaccharide primary structure. In order to fully understand the molecular basis of these recognition events, the three-dimensional structure of the carbohydrate chains of glycopeptides must be determined.

The synthesis of Asn-linked oligosaccharides is regulated by a highly specific sequence of events. The type of carbohydrate chain that is eventually synthesized appears to be controlled by a complex interaction between the polypeptide sequence and the relative levels of activity of certain transferases. For example, two well-characterized enzymes are GlcNAc-transferase I and GlcNAc-transferase III (Harpaz & Schachter, 1980; Narasimhan, 1982). The action of the former is an essential requirement for processing of the carbohydrate chain to occur. The action of the GlcNAc-transferase III, on the other hand, is highly inhibitory to the subsequent action of at least four other enzymes in the pathway despite the fact that they act at sites remote from the point of substitution by GlcNAc-transferase III. Thus, it is essential to determine the three-dimensional structure of these substrates

```
                                            COMPLEX AND BISECTED COMPLEX
6G       6GN2       6i              F
Galβ1-4GlcNAcβ1-2Manα1-6          Fucα1-6
                          \              \
                    R-4Manβ1-4GlcNAcβ1-4GlcNAcβ1-Asn    GGN:      R = HO-
                    /  4i    core          Asn          GGN(GN):  R = GlcNAcβ1-
        GlcNAcβ1-2Manα1-3    GN            GN                            bis GN
        3GN2      3i,3t


                                            HIGH MANNOSE AND HYBRID
6t   Manα1-6
           \   6i
3t   Manα1-3Manα1-6
                  \
            Manβ1-4GlcNAcβ1-4GlcNAcβ1-Asn    E3:    R' = HO-
            /  4i    core       Asn          D3:    R' = Manα-  2t
   R'-2Manα1-3      GN         GN            GNM₅:  R' = GlcNAcβ1-
          3i                                               GN2


                                            BISECTED HYBRID
6t   Manα1-6
           \   6i
3t   Manα1-3Manα1-6
                  \
bis GN  GlcNAcβ1-4Manβ1-4GlcNAcβ1-4GlcNAcβ1-Asn    C3B:  R'' = HO-
            /  4i    core           Asn            A3:   R'' = Galβ1-4GlcNAcβ1-
   GlcNAcβ1-2Manα1-3    GN          GN
   GN2      /  3i
        R''-4
```

FIGURE 1: Structures and nomenclature of asparaginyl oligosaccharides. The shorthand notation for the structures and for the residues is taken from Carver & Grey (1981).

in order to understand the molecular basis of this specificity.

In this and the following paper (Brisson & Carver, 1983a), the solution conformation is presented for representatives of each of the major classes of asparaginyl oligosaccharides (high mannose, bisected hybrid, complex, and bisected complex) (Carver & Grey, 1981). In this report the conformation of $\alpha(1-3)$-, $\alpha(1-2)$-, $\beta(1-2)$-, and $\beta(1-4)$-linked units is described, and in the following report the conformation of the $\alpha(1-6)$-linked moiety is discussed. The conformational properties of these glycopeptides were determined by high-resolution ^{1}H nuclear magnetic resonance in conjunction with potential energy calculations. The NMR parameters that were used in this analysis were chemical shifts and nuclear Overhauser enhancements (NOE). Potential energy calculations were used to evaluate the preferred conformers available for the different linkages in glycopeptides and to draw conclusions about the behavior in solution of these molecules.

In order to interpret the chemical shifts of these high molecular weight oligosaccharides, smaller model compounds that are an integral part of these molecules had previously been synthesized. Since their ^{1}H NMR spectra were much less complex than those of the N-linked oligosaccharides, their complete assignment was possible (Winnik et al., 1982a,b; Brisson & Carver, 1982). These assignments were then used to identify unknown resonances in the spectra of asparaginyl oligosaccharides. A detailed comparison of the chemical shifts of these compounds was used to detect long-range interactions between two residues that are remote in the primary structure (Carver & Grey, 1981; Brisson & Carver, 1982). These perturbations can only arise if the two residues are in close proximity to one another. Nuclear Overhauser enhancements were also used in this analysis because the magnitude of this effect depends, along with other factors, on the relative disposition of the protons in the molecule and thus on the three-dimensional structure. The use of these techniques to determine the preferred conformations of a methyl manno-

trioside which is an integral part of N-linked oligosaccharides has been previously described (Brisson & Carver, 1983b). NOE measurements have also been applied to the determination of the sequence of sugars in glycopeptides (Brisson & Carver, 1983c).

Experimental Procedures

Samples were prepared in D_2O as previously described (Brisson & Carver, 1983b). The NOE spectra and spin-tickled spectra (low-power decoupling) were obtained by difference spectroscopy under conditions which have also been described previously (Brisson & Carver, 1983b).

Figure 1 displays the structures of the compounds and the symbols used to represent them. Throughout this paper, the nomenclature of Carver & Grey (1981) has been used to designate the various residues within the structure. Hence the mannose residues are identified by a single number representing their linkage, i.e., 4 for Manβ1-4, 6 for Manα1-6, etc. A "t" or "i" is added to indicate whether the residue is terminal (nonreducing) or internal; i.e., 4i represents the internal-substituted Manβ1-4 residue. The other residues are identified by capital letters (GN for GlcNAc, G for Gal, and F for Fuc) with a number of their linkage, i.e., GN2. The anomeric configuration is not included in these symbols because it is clear from the context whether the linkage is α or β. Since all the structures of Figure 1 contain the unit $Man_3GlcNAc_2Asn$, the Man_3 component is referred to as the mannotriose unit, the GlcNAc linked to Asn as the Asn GN, and the other one as the core GN. The branches on the mannotriose unit are referred to as the 3-arm and the 6-arm. In the structure where the unit GlcNAcβ1-4Manβ occurs, this GlcNAc is called the bisecting GlcNAc which is abbreviated as bis GN. In complex structures, to indicate on which arm of the mannotriose unit a residue is located, a number representing the linkage at the
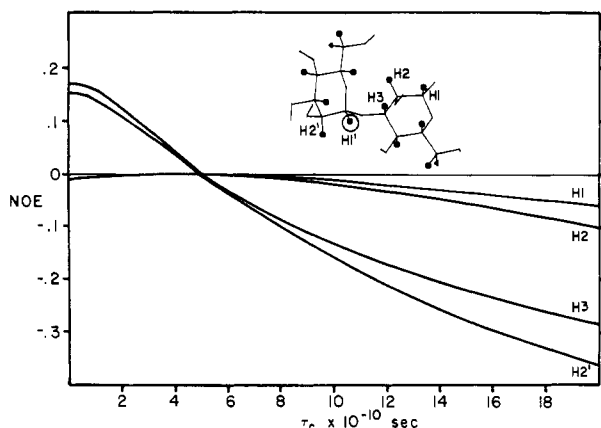
FIGURE 2: Variation of the ^{1}H-^{1}H NOE (360 MHz) as a function of the correlation time τ_c. For methyl mannobiosides and a methyl mannotrioside, $\tau_c = (1-1.5) \times 10^{-10}$ s (Brisson & Carver, 1982b). For the asparaginyl oligosaccharides, τ_c is between 8×10^{-10} and 12×10^{-10} s.

branch point precedes the name of the residue. As an example, *3*GN2 specifies GlcNAcβ1-2 on the 3-arm.

The geometry of the individual sugar rings in the glycopeptides was assumed to be in a normal $^4C_1$ chair conformation. This assumption is supported by the fact that the proton vicinal coupling constants observed in model compounds were not changed by various substitutions of the ring (Brisson & Carver, 1983b). Since the ring conformations are fixed, the three-dimensional structure of the carbohydrate chain of a glycopeptide will depend on the value of the torsional angles around the glycosidic bonds, ϕ and ψ. For a 1-6 linkage, the orientation of the substituted hydroxymethyl group about the C5-C6 bond also needs to be determined (Tvaroska et al., 1978).

The molecular modeling and NOE calculations were carried out as previously described (Brisson & Carver, 1983b). In brief, the coordinates of the oligosaccharides were generated from those of monosaccharides (Rees & Skerett, 1970) and calculated as a function of the torsional angles about the glycosidic bonds. Atomic coordinates for αMan were generated from neutron diffraction data (Jeffrey et al., 1977). X-ray data were used to generate the coordinates for βMan (Warin et al., 1979), βGlcNAc (Mo, 1979), βGal (Fries et al., 1971), and αFuc (Cook & Bugg, 1975). Glycosidic bond angles were also taken from solid-state data when available: Manα1-3 and Manβ1-4 (Warin et al., 1979), GlcNAcβ1-4 (Mo, 1979), Galβ1-4 (Fries et al., 1971), and Manα1-6 (Arnott & Scott, 1972). All other glycosidic bond angles were set to 117.5° (Biswas & Rao, 1981). For the coordinates obtained from X-ray data, every C-H bond was oriented at 109.5° with respect to the two adjacent bonds in the pyranose ring with a C-H distance of 1.10 Å.

The NOE's were calculated by solving algebraically the equations described by Noggle & Shirmer (1971). The potential energy was computed by considering van der Waals interactions (hard sphere) between nonbonded atoms (Lemieux et al., 1980) and electrostatic energy terms (Potenzone & Hopfinger, 1975). The influence of the exoanomeric effect on conformational equilibrium was also included (Thogersen et al., 1982).

Apart from depending on interproton distances, the sign and magnitude of an NOE depends on the Larmor frequency of the hydrogen nuclei (ω_0) and on the correlation time (τ_c) of the protons involved (Noggle & Schirmer, 1971). Such a dependence is shown in Figure 2 for the Manα1-3Manβ1- unit. From the magnitude of an *intra*residue NOE (e.g., the

NOE on H2' upon saturation of H1'), the tumbling time of the molecules can be estimated. For methyl mannobiosides and methyl mannotriosides, tumbling times near $\sim 1.5 \times 10^{-10}$ s were found (Brisson & Carver, 1983b), while for the parent asparaginyl oligosaccharides, tumbling times near 10×10^{-10} s occur. The longer tumbling times in asparaginyl oligosaccharides lead to the appearance of NOE's that were not observed in the oligomannosides. For example on saturation of H1' in the Manα1-3Manβ1- unit of asparaginyl oligosaccharides, small negative NOE's for H1 and H2 were detected which were not observed for the oligomannosides (Figure 2 and Figure 4). Thus, it is important to distinguish NOE's that are due to a change in linkage conformation from those that are a natural consequence of the longer tumbling time of the molecule.

The correlation time of a proton will be affected by the size and shape of the molecule and internal motion about the glycosidic bonds. Since asparaginyl oligosaccharides are not completely globular, anisotropic tumbling is expected to affect the magnitudes of the enhancements. Fast internal motion about the glycosidic bonds would also be expected to decrease the magnitude of the observed NOE. From ^{13}C NMR studies on disaccharides and trisaccharides, the internal rates of motion were determined to be slower than the overall tumbling rate of the molecule and were considered to be restricted to vibrational motion about a stable conformer (Brisson & Carver, 1983b; Hayes et al., 1982). Since in asparaginyl oligosaccharides the overall tumbling rate of the molecule is slower than those of disaccharides by a factor of 10, internal motions might have a more pronounced effect. For the asparaginyl oligosaccharides and the present field strength, ^{13}C or ^{1}H spin-lattice relaxation times (T_1) were not sensitive to molecular motions since $\omega_0\tau_c$ is close to 1 and the T_1 values passed through shallow minima (Sykes et al., 1978; Doddrell et al., 1972). Since, even for isolated resonances, the line widths of ^{1}H resonances are affected by virtual coupling effects (Brisson & Carver, 1982), T_2 values obtained from such measurements were not used as a gauge of internal mobility. However, from the magnitude of *intra*residue NOE's observed in asparaginyl oligosaccharides (Table II), the correlation times for various protons in E3 were estimated to be from $(8 \pm 2) \times 10^{-10}$ to $(12 \pm 3) \times 10^{-10}$ s, indicating that the effects due to anisotropic tumbling or internal motion were minimal. Similar conclusions applied to the other asparaginyl oligosaccharides. To compare NOE's from different molecules and to minimize errors due to variation in τ_c within a molecule, relative NOE's (ratio of two NOE's), which do not vary significantly for the above range of τ_c (Figure 2), were used in the analysis of the NOE data, along with an average tumbling time of 10×10^{-10} s.

Assignments. Selected samples of the NOE difference spectra for the asparaginyl oligosaccharides E3, D3, A3, GGN, and GGN(GN) (see Figure 1 for structures and nomenclature) are shown in Figures 3, 4, 7, and 10. The spectra for C3B are not shown since they were similar to those of A3. By the nature of the NOE effect only protons in close proximity to the saturated proton experienced any significant enhancement. In weakly coupled systems of βGlcNAc, βMan, or βGal, three significant intraresidue NOE's (greater than −10%) were generally observed. One of these was assigned to H2 by spin tickling. The other two NOE's were identified as H3 and H5 based on a comparison of their chemical shifts and multiplicity with those of model compounds (Winnik et al., 1982a; Brisson & Carver, 1982; Dorland et al., 1977). For αMan, the major NOE on saturation of H1 was on H2. However, because the Man H2 resonances were isolated from other resonances, NOE

Table I: First-Order Chemical Shifts of Asparaginyl Oligosaccharides[a]

residue[b]	H1	H2	H3	H4	H5	H6	H6'
4i							
E3	4.784	4.255	3.77	3.77	3.63	3.77	3.96
D3	4.772	4.234	3.75	3.77	3.63	3.77	3.96
GNM$_s$	4.779	4.247	3.77	3.77	3.65	3.77	3.96
C3B	4.741	4.188	3.88	3.88	3.65	3.89	3.89
GGN	4.766	4.253	3.77	3.77	3.63	3.79	3.96
GGN(GN)	4.685	4.173	3.867	4.077	3.53	3.90	3.90
3-arm 3i, 3t							
E3	5.092	4.072	3.890	3.62	3.78		
D3	5.338	4.119	4.007				
GNM$_s$	5.110	4.197	3.905				
C3B	5.055	4.255	3.892		3.78		
GGN	5.115	4.188	3.901				
GGN(GN)	5.057	4.253	3.883		3.73		
2t							
D3	5.053	4.063	3.880				
3GN2							
GNM$_s$	4.553	3.696	3.57	3.45	3.45		
C3B	4.532	3.716	3.60	3.47	3.47		
GGN	4.553	3.690	3.57	3.44	3.44		
GGN(GN)	4.556	3.710	3.60	3.47	3.47		
6i							
E3	4.873	4.145	3.90	3.90	3.86	3.73	3.96
D3	4.871	4.146					
GNM$_s$	4.870	4.143	3.89	3.89		3.77	
C3B	4.918	4.162	3.89	3.89	3.76	3.76	
GGN	4.926	4.108	3.890				
GGN(GN)	5.013	4.136	3.828				
6-arm 3t							
E3	5.092	4.067	3.890	3.62	3.78		3.78
D3	5.089	4.063	3.890				
GNM$_s$	5.084	4.061	3.887		3.78		3.78
C3B	5.038	4.061	3.880		3.78		3.78
6t							
E3	4.908	3.983	3.840				
D3	4.908	3.988	3.840				
GNM$_s$	4.904	3.984	3.840				
C3B	4.929	4.005	3.862				
6GN2							
GGN	4.581	3.741	3.77	3.74	3.62		
GGN(GN)	4.579	3.738	3.63	3.74	3.51		
6Gal							
GGN	4.471	3.538	3.68	3.92	3.72		
GGN(GN)	4.471	3.54					
bis GN							
C3B	4.410	3.693	3.573	3.253	3.440		
GGN(GN)	4.465	3.694	3.567	3.260	3.403		3.68
core GN							
E3,D3	4.603	3.77	3.77	3.76	3.62		
GNM$_s$	4.600	3.79	3.79				
C3B	4.588	3.78	3.78	3.78			
GGN	4.682	3.77	3.73	3.73	3.59		
GGN(GN)	4.674	3.805					
Asn GN							
E3,D3,C3B	5.073	3.86	3.77	3.66	3.60		
GGN,GGN(GN)	5.071	3.854	3.73	3.71	3.71		
Fuc							
GGN	4.873	3.78	3.87	3.80	4.13	1.210	
GGN(GN)	4.881	3.78		3.75	4.14	1.197	

[a] In ppm, at 23 °C, with internal acetone set at 2.225 ppm. [b] See Figure 1 for nomenclature.

or spin-tickling experiments on the Man H2 resonances could be used to detect the Man H3 signals. Interresidue NOE's were assigned on the basis of studies performed in model compounds (Brisson & Carver, 1982, 1983b).

When the chemical shift difference between coupled resonances approached the magnitude of the coupling constants (strong coupling), a distortion of the multiplets from the expected first-order pattern resulted. For example, on saturation of the H1 of the Manα1–3 residue in GGN (Figure 4d), the distorted signal at 3.77 ppm can only arise from the strongly coupled H3 and H4 resonances of the Manβ1–4 residue. Whereas for GGN(GN), on saturation of the H1 of the

Manα1–3 residue (Figure 4e), the NOE at 3.867 ppm was assigned to the H3 resonance of the Manβ1–4 residue, since this signal had the expected weakly coupled pattern. Hence, due to strong coupling, additional resonances could be located.

The proposed assignments for the resonances observed in the NOE difference spectra are presented in Table I. The assignments for A3 are not given since they were not used in the following discussion. The agreement between the calculated NOE's and the observed NOE's (Table II) confirmed the assignments in Table I. However, whenever necessary, the details of the assignments will be given in the following sections. The chemical shifts for the 6-arm will be discussed

Table II: Relative Nuclear Overhauser Enhancements[a] for the Manα1-3Man Unit and for the Bisecting GlcNAc

GlcNAcβ1-2Manα1-3Man Unit: Saturated Signal = Manα1-3 H1

	Manα1-3		-3Man			GlcNAc1-2
	H2	H3	H1	H2	H3-H4	H1
(GGN), obsd	[0.11]	0.5	0.3	0.4	2.3	0.9
(GGN), calcd	1.0	0.8	0.1	0.2	1.3	1.0

Manα1-3Man Unit in E3 or GlcNAcβ1-2Manα1-3Man Unit in GGN(GN): Saturated Signal = -3Man H2

	-3Man		Manα1-3	
	H1	H3	H1	H5
E3, obsd	[0.09]	0.8	0.1	0.8
E3, calcd	1.0	1.4	0.2	1.4
GGN(GN), obsd	[0.08]	1.3	0.4	2.8
GGN(GN), calcd	1.0	1.3	0.3	2.7

Bisecting GlcNAc: Saturated Signal = Bisecting GlcNAc H1

	bisecting GlcNAc				Manβ1-4		Manα1-6			Manα1-3	
	H5	H2	H3	H4	H3-H4, H5-H6'	H2	H2	H1	H5, H6	H1	H2
A3, obsd	[0.24]	0.2	0.7	0.2	1.5	0.2[b]	0.1	0.3	0.1	0.2
A3, calcd	1.0	0.3	0.8	0.1	1.7	0.1[b]	0.1	0.1	0.1	0.0
					H4						
GGN(GN), obsd	[0.20]			0.2	1.0			0.1		0.1	
GGN(GN), calcd	1.0	0.3	0.8	0.2	1.0			0.1		0.1	

Bisecting GlcNAc: Saturated Signal = Bisecting GlcNAc H4

	bisecting GlcNAc					Manα1-3	GlcNAcβ1-2
	H2	H5	H3	H1	H6'	H2	H5
GGN(GN), obsd	[0.15]	0.5	1.0	0.2		0.1	0.4
GGN(GN), calcd	1.0	0.4	0.6	0.2	0.3	0.0	0.4

[a] The absolute NOE (observed), indicated by brackets, is given for the reference signal. The linkage conformations given in Table V were used for the NOE calculations. [b] These numbers encompassing more than one proton represent overlapping NOE's for these protons.

later (Brisson & Carver, 1983a).

Results and Discussion

In order to investigate differences in conformation in the Man₃GlcNAc₂ core brought about by various substitutions on that core, the NOE patterns for the four major classes of asparaginyl oligosaccharides were compared. Changes in orientation about the 3-arm or 6-arm should lead to large differences in the NOE pattern and to large differences in chemical shift between these structures. In section A, the conformation of the Manα1-3Man unit present in asparaginyl oligosaccharides will be discussed. In sections B, C, and D the linkage conformation for Manα1-2, GlcNAcβ1-2, and the bisecting GlcNAc will be presented. The effect of these substitutions on the 3-arm orientation will also be discussed in each section. In the following paper the conformation of the 6-arm will be presented.

(A) Manα1-3 Linkage. In a previous study, the α1-3 linkage conformation for Manα1-3Manα1-OMe was found to be (-45 ± 15°, -15 ± 15°) (Brisson & Carver, 1983b). Two NOE experiments were used to estimate the linkage conformation: (i) saturation of the H2 resonances of the aglycon (i.e., -3Man) and (ii) saturation of the H1 resonance of the glycon (Manα1-3). In the first case, saturation of the aglyconic H2 resulted in NOE's on the aglyconic H1 and H3 and the glyconic H5-H6' resonances (Figure 3a). In the high mannose structure E3, on saturation of 6i H2, NOE's on 3t H5-H6' (3.78 ppm) and 6i H3-H4-H5 (broad complex near 3.9 ppm) are observed. A similar NOE pattern was observed for saturation of 6i H2 in D3 (not shown), saturation of 6i H2 and 4i H2 in A3 (Figure 3c), and saturation of 4i H2 in GGN(GN) (Figure 3d). In high mannose and complex structures, on saturation of 4i H2, the NOE's on 3i H5 and
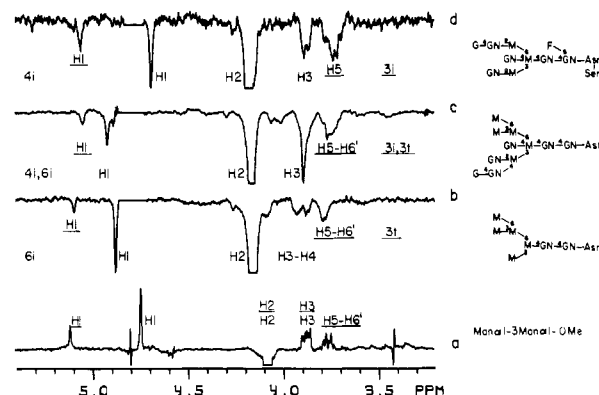

FIGURE 3: NOE difference spectra on saturation of the aglyconic H2 in the Manα1-3Man unit in (a) Manα1-3Manα1-OMe, (b) E3, (c) A3, and (d) GGN(GN). The largest NOE has been set to full scale for all these spectra. The interresidue NOE's are underlined. The resonances belonging to the same residue and the residue symbol are usually located on the same horizontal line. Hence, in (b), on saturation of 6i H2 intraresidue NOE's are observed on 6i H1 and H3-H4 and interresidues NOE's are observed on 3t H1 and H5-H6'.

on 4i H3 overlap, and therefore their individual signals could not be distinguished.

In the second case, saturation of the Manα1-3 H1 in the disaccharide produced a major NOE on the H3 of the aglycon (Figure 4a). In the asparaginyl oligosaccharides, this pattern was also observed (Figure 4b-e). However, except for GGN and D3, because of overlap, the Manα1-3 H1 and the Asn GN H1 resonances were saturated simultaneously, and a more complicated NOE spectrum ensued. The additional NOE's arising from the saturation of Asn GN H1 are indicated by "stars" in Figure 4. Despite these extra NOE's, the en-
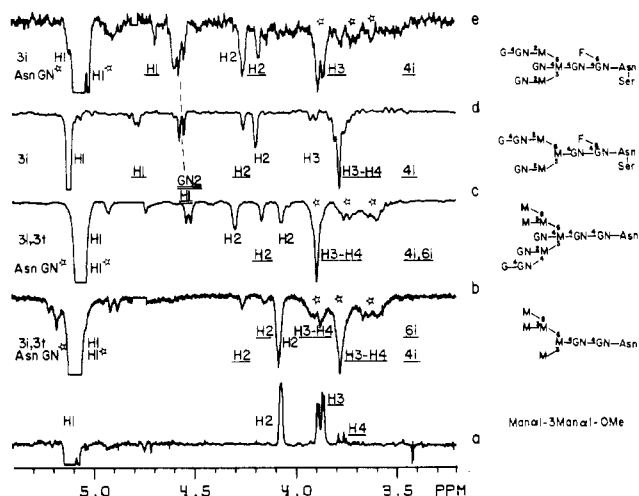
FIGURE 4: NOE difference spectra on saturation of Manα1–3 H1 in (a) Manα1–3Manα1–OMe, (b) E3, (c) A3, (d) GGN, and (e) GGN(GN). The stars represent interfering NOE's due to simultaneous saturation of Asn GN H1.

Table III: NOE's for the Manα1–2Man Unit in D3

saturated signal	obsd signal	NOE absolute obsd	NOE relative obsd	NOE relative calcd[a]
3i H1	3i H2	0.07	1.0	1.0
	2t H1	0.01	0.3	0.3
	2t H2	0.00	0.0	0.1
	4i H1			0.1
	4i H2	0.03	0.4	0.1
	4i H3,H4	0.16	2.3	1.2[b]
3i H2	3i H1	0.04	1.0	1.0
	3i H3	0.09	2.3	2.3
	2t H1	0.07	1.8	2.1
	2t H2			0.4
2t H1	2t H2	0.04	1.0	1.0
	3i H1	0.005	0.1	0.1
	3i H2	0.03	0.8	0.7

[a] $(\phi, \psi) = (-50, -20)$. [b] An NOE for 2t H5 (2.25 Å from 3i H1), which cannot be distinguished from the NOE on 4i H3 due to overlap, is expected to increase the calculated ratio to 2.7.
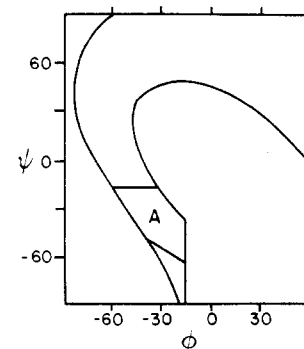

FIGURE 5: Contour map for NOE's in the Manα1–2Man unit. A contour map represents the values of ϕ and ψ for which the computed NOE values were within error bounds ($\pm 40\%$) of the experimental measurement (Table III). Only the complete contour map for the relative NOE of [3i H2/2t H2] (0.8 $\pm$ 40%) on saturation of 2t H1 is shown. The intersection of this band with the contour map generated for the relative NOE of [2t H1/3i H1] (1.8 $\pm$ 40%) on saturation of 3i H2 is denoted by area A. The other measurements in Table III did not further restrict area A.

hancement for 4i H3 could be readily recognized since H3 was strongly coupled with H4 [except for GGN(GN) in Figure 4e]. In high mannose and bisected hybrid structures (Figure 4b,c) the H1 resonances of both Manα1–3 residues, as well as that of the Asn GN, were simultaneously saturated with the result that NOE's are observed on (i) 4i H2 and H3–H4 (overlapping with an NOE on Asn GN H3), (ii) 6i H2 and 6i H3–H4 (overlapping with a weak NOE on Asn GN H2), and (iii) Asn GN H4–H5. In E3 (Figure 4b) the chemical shift difference between 6i H3 and 6i H4 is bigger than that for 4i H3 and 4i H4 since the H3–H4 complex of 6i is broader than for 4i. However, in A3 (Figure 4c), the NOE's on H3–H4 of 4i and 6i overlap near 3.88 ppm. For all the asparaginyl oligosaccharides, small interresidue NOE's on H2 and H1 of the aglycon (4i or 6i) are also observed, as expected (Figure 2 and Table II).

Since, similar NOE patterns were observed for the Manα1–3Man unit in all the asparaginyl oligosaccharides, the α1–3 linkage conformation in each case should be the same as for a terminal Manα1–3 residue in the methyl mannobioside (Brisson & Carver, 1983b). Therefore, neither a substitution at C2 or C4 by βGlcNAc or C2 by αMan nor the proximity of bis GN had a major influence on the orientation of the 3-arm of the mannotriose unit. This point will be discussed further in the next sections where the linkage conformations for Manα1–2, GlcNAcβ1–2, and the bisecting GlcNAc are determined.

(B) Manα1–2 Linkage. The linkage conformation for the Manα1–2Man unit was determined from NOE experiments on D3 (Figure 1). Because all the H1 and H2 resonances are isolated from each other, the interpretation of the NOE spectra on saturation of the Man H1 or H2 resonance was straightforward (Table III). When contour maps which show the allowed (ϕ, ψ) angles for which the computed NOE values fall within the error bounds of the observed values (Brisson & Carver, 1983b) were generated, the linkage conformation was determined (Figure 5). An error bound of $\pm 40\%$ was used on the relative NOE values to take into account errors involved in the estimation of τ_c and errors in the measurements themselves. Nonetheless, the linkage conformation was determined within $\pm 20°$, with $\phi = -45°$ and $\psi = 20°$. These results agree with potential energy calculations which predict a minimum near ($-50°$, $-20°$) for the α1–2 linkage in the Manα1–2αManα1–3Manβ1– unit.

Some large chemical shift perturbations arise from the substitution by αMan at C2 on the Manα1–3 residue (Cohen & Ballou, 1980; van Halbeek et al., 1980; Carver et al., 1981; Carver & Grey, 1981; Ogawa & Yamamoto, 1982). A stereo diagram of the Manα1–2Manα1–3Manβ1– unit is shown in Figure 6a. The proximity of the ring oxygen and O6 of the Manα1–2 residue to 3i H1 (3–3.5 Å) is the probable cause of the downfield shift of 0.256 ppm experienced by the H1 resonance of the Manα1–3 residue upon a substitution at C2 (E3 and D3 in Table I). Another large downfield shift (0.117 ppm) is observed for H3 of the Manα1–3 residue. The likely origin of this shift is the reorientation of the neighboring O3-H of the Manα1–3 residue, since for certain orientations of the hydroxyl group, the hydrogen atom of O3-H is in contact with H1 of the Manα1–2 residue. This mechanism of long-range perturbation brought about by the reorientation of hydroxyl groups upon a substitution has been termed "conformational transmission" by Dabrowski et al. (1980).

The linkage conformation of ($-50°$, $-20°$) predicted for the α1–3 linkage by potential energy calculations on the Manα1–2Manα1–3Manβ1– unit support the earlier conclusion (section A) that the Manα1–3 orientation is not appreciably affected by a substitution at C2.

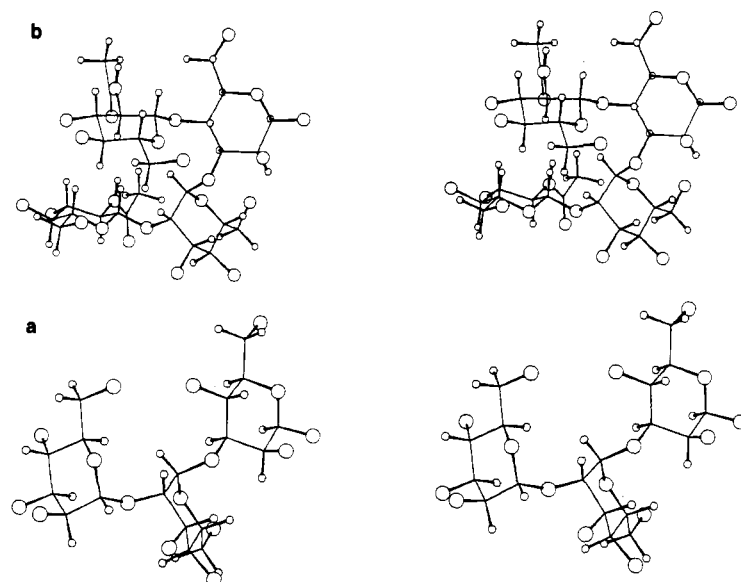(C) GlcNAcβ1–2 Linkage. Three different NOE experiments were performed to determine the linkage conformation

b

a

FIGURE 6: Stereo diagrams for the 3-arm in D3 and bisected structures: (a) Manα1-2Manα1-3Manβ1- and (b) GlcNAcβ1-2Manα1-3-(GlcNAcβ1-4)Manβ1-. The large spheres are oxygen atoms and the small ones are hydrogen atoms. Hydrogen atoms of hydroxyl groups are not shown. The βMan residue is located on the right hand side of the projection. The linkage conformations that have been used are given in Table V.

Table IV: NOE's for the GlcNAcβ1-2Man Unit

| saturated signal | rel NOE[b] | compound | | | | | av | calcd[a] |
		GGN	GNGN	GGN(GN)	C3B	A3		
3i H1	GN2 H1/3i H2	0.9	1.2	1.0	1.2	1.1	1.1	1.1
6i H1	GN2 H1/6i H2	0.9	0.8	1.5				
3i H2	GN2 H1/3i H1	0.8	1.3	0.5	0.8	0.9	1.0	1.0
6i H2	GN2 H1/6i H1	1.3	1.0	1.0				
3GN2 H1	3i H2/3i H1	0.8	0.6	1.0	1.0		1.1	0.9
6GN2 H1	6i H2/6i H1	1.1	1.0	1.4				

^{a} $(\phi, \psi) = (40°, 30°)$. ^{b} Ratio of NOE's as shown.

in the GlcNAcβ1-2Man unit: saturation of Man H1, Man H2, or GN2 H1 (Table IV). These experiments were carried out for five different compounds containing GN2 located either on the 3-arm or 6-arm. Since the NOE data were similar for GG compared to GGN and A3 compared to C3B, respectively, neither a substitution at C4 of GN2 or at C4 of 3i nor the presence of the bis GN had an appreciable effect on the conformational properties of the β1-2 linkage. The average values for the three distinct NOE experiments were used to determine the linkage conformation in order to compensate for possible differences in anisotropic tumbling which might arise for GN2 residues located in different parts of the molecule (i.e., on the 3-arm vs. the 6-arm). From the common area found upon the superposition of the contour maps generated from the three separate NOE measurements, the torsion angles for a β1-2 linkage were determined to be within 30–60° for φ and within 25–35° for ψ (Figure 7). A linkage conformation of (40°, 30°) was found to give the best fit to the data presented in Table IV. These results are consistent with potential energy calculations for this linkage in the GlcNAcβ1-2Manα1-3Manβ1- unit, since the range of experimentally deduced angles overlapped with a broad energy minimum occurring near (50–55°, 10–25°). The minimum energy conformer for the α1-3 linkage in the GlcNAcManα1-3Manβ1- unit is also the same as for a terminal Manα1-3 residue (Table V), supporting the earlier conclusion that the orientation of the Manα1-3 residue is not appreciably affected by a substitution at its C2 by βGlcNAc (section A).

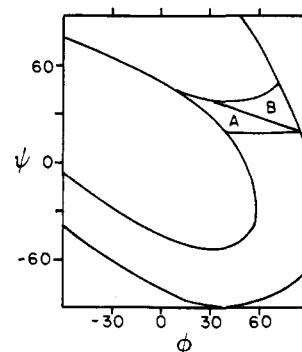FIGURE 7: Contour map for NOE's in the GlcNAcβ1-2Man unit. A contour map represents the values of φ and ψ for which the computed NOE values were within error bounds (±40%) of the experimental measurement (Table IV). Only the complete contour map for the relative NOE of [GN2 H1/Man H1] (1.0 ± 40%) on saturation of Man H2 is shown. Man represents 3i or 6i. Areas A and B represent the intersection of this band with the band generated from the relative NOE of [GN2 H1/Man H2] (1.1 ● 40%) on saturation of Man H1. The relative NOE of [Man H2/Man H1] (1.1 ± 40%) on saturation of GN2 H1 restricts the allowed linkage conformations to area A.

(D) Bisecting GlcNAc Linkage. Despite the large chemical shift perturbations on 3i (Table I) caused by the presence of the bisecting GlcNAc, it was found to have no major effect on the orientation of the 3-arm. In order to explore the possible origin of these perturbations, the linkage conformation for the bisecting GlcNAc was determined from NOE experiments
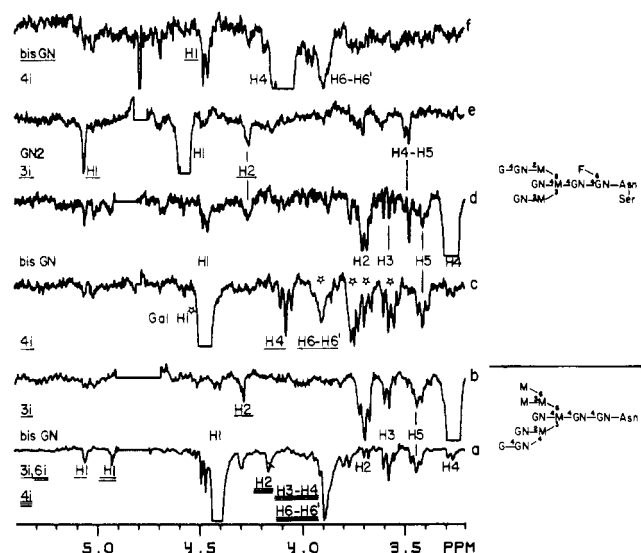
FIGURE 8: NOE difference spectra used to determine the linkage conformation of the bisecting GlcNAc. The spectra for saturation of the following resonances are shown: (a) bis GN H1 of A3, (b) bis GN H4 of A3, (c) bis GN H1 of GGN(GN) (the stars denote interfering NOE's arising from the simultaneous saturation of Gal H1), (d) bis GN H4 of GGN(GN), (e) 3GN2 H1 of GGN(GN), and (f) 4i H4 of GGN(GN).
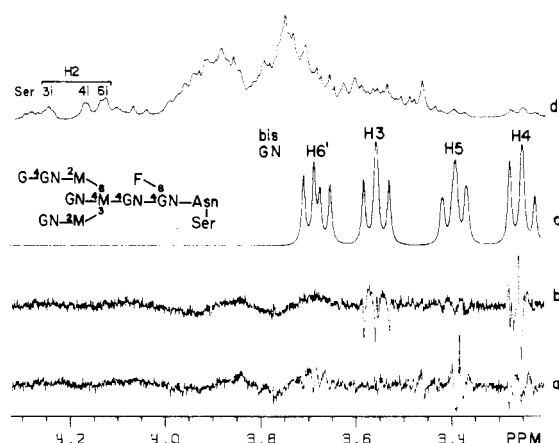

FIGURE 9: Spectral patterns for the bisecting GlcNAc: (a) Spin tickling of H5 to detect the vicinally coupled H4 and H6' resonances. The H6 resonance is not sufficiently perturbed to be detected. (b) Spin tickling of H4 to detect the H3 and H5 resonances. (c) Simulated spectrum: the H2 resonances which can be located by spin tickling of H1 is not shown since it would overlap with the H6' resonance and complicate the simulated spectrum. (d) Normal spectrum of GGN-(GN).

performed on a bisected complex structure [GGN(GN)] and two bisected hybrid structures (C3B and A3) (Figure 1). The ^1H chemical shifts assignments are first discussed, and then interresidue NOE's, which help define the orientation of the bisecting GlcNAc with respect to the 3-arm, are presented. The chemical shifts for bisected structures and the NOE data are then interpreted in terms of the minimum energy conformer determined from potential energy calculations.

Chemical Shifts. The assignment for the proton resonances of the bis GN (Table I) was obtained from NOE and spin-tickling experiments (Figures 8 and 9). As expected (Table II), saturation of bis GN H1 leads to large intraresidue NOE's on H3 and H5 and to smaller ones on H2 and H4 (Figure 8a,c). For A3, the NOE at 3.9 ppm is due to an interresidue NOE on the 4i H3–H4 and 4i H6–H6' signals. In GGN(GN), the NOE spectrum on saturation of bis GN H1 was complicated by the appearance of additional NOE's (denoted by

Table V: Linkage Conformations for the 3-Arm of Asparaginyl Oligosaccharides

	(ϕ, ψ) (deg, deg)
Manα1–3Man	(−50, −10)
Manα1–3Man	(−50, −20)
Manα1–2	(−50, −20)
Manα1–3Man	(−50, −10)
GlcNAcβ1–2	(40, 30)
GlcNAcβ1–4Man	(60, 10)
Manα1–3	(−50, −20)
GlcNAcβ1–2	(40, 30)

"stars") due to the simultaneous saturation of Gal H1 (Figure 8c). The assignment of the NOE's resulting from saturation of Gal H1 was obtained from the NOE spectrum for saturation of the isolated Gal H1 resonance in GGN (Table I). For GGN(GN) the NOE pattern for 4i H4 and H6–H6' was drastically different from that of A3. These changes arise from the different orientation of the 6-arm between bisected complex and bisected hybrid structures (Brisson & Carver, 1983a). The NOE pattern (Figure 8b,d) obtained on saturation of the isolated bis GN H4 resonance permitted the detection of the bis GN H1, H2, H3, and H5 resonances (Table II), thus confirming the assignments proposed from the NOE pattern obtained on saturation of bis GN H1 (Figure 8a,c). Spin tickling of bis GN H4 in GGN(GN) (Figure 9b) also confirmed these assignments. Spin tickling of the isolated H5 resonance (3.403 ppm) led to the detection of the H6' signal (3.68 ppm). The vicinal coupling constants between H1, H2, H3, H4, and H5 were found to be the same as for a terminal GlcNAc in a chitobioside, indicating that the bis GN ring was not distorted from a normal chair conformation. A value of 8.0 Hz for $J_{5,6'}$ was necessary to simulate correctly the H5 and H6' signals (Figure 9d). Since, for a terminal GlcNAc residue, $J_{5,6'}$ is usually 5.5 Hz, the hydroxymethyl group of the bis GN must be restricted to the rotamer with $\omega = -60°$ (Brisson & Carver, 1983b).

Interresidue NOE's. On saturation of bis GN H1, small NOE's (0.02) were observed on 3i H1, 6i H1, and 6i H2 (Figure 8a). A small interresidue NOE was also observed on 3i H2 on saturation of bis GN H4 (Figure 8b,d). In GGN-(GN) an interresidue NOE was also observed at 3.49 ppm (Figure 8d). In A3, it was difficult to assess whether this NOE was present due to interference from the bis GN H5 resonance. These interresidue NOE's can only arise from the close proximity of these residues to one another. Since these NOE's are qualitative, the previous approach used to determine the linkage conformation is not applicable in this case, and one must resort to potential energy calculations in order to interpret these results.

Potential Energy Calculations. The nonbonded and electrostatic potential energy for the GlcNAcβ1–2Manα1–3-(GlcNAcβ1–4)Manβ unit was calculated by keeping the GlcNAcβ1–2 linkage conformation fixed at (40°, 30°) since, within experimental error, the NOE pattern for this unit was similar to that observed in unbisected structures (Table IV). The linkage conformation for the Manα1–3 and bisecting GlcNAc residues was set initially at (−50°, −10°) and (50°, 0°), respectively, and the torsional angles were then varied ±40° in steps of 10°. Variations outside this range were not energetically favorable due to severe contacts between the various residues in the structure. The orientations of the hydroxymethyl groups were kept fixed at $\omega = -60°$, since for the bisecting GlcNAc, the large $J_{5,6'}$ implied that this rotamer was highly populated in solution. A minimum was found at
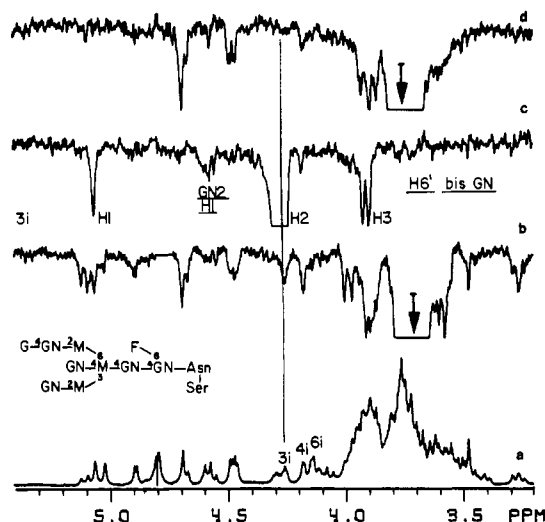
FIGURE 10: NOE between the H2 of the Manα1–3 residue and H6′ of the bisecting GlcNAc. (a) Normal spectrum of the bisected complex structure GGN(GN). NOE difference spectra for (b) bis GN H6′ saturated, (c) 3i H2 saturated, and (d) irradiation 10 Hz downfield of the point of irradiation in (b).

(−50°, −20°) and (60°, 10°) for the Manα1–3 and the bisecting GlcNAc linkages, respectively. A number of conformers within 1 kcal/mol could be found within ±10° of this minimum, indicating that no major reorientation of the 3-arm was necessary to accommodate the bisecting GlcNAc. A stereo diagram of the minimum energy conformer (Table V) is shown in Figure 6b. As can be observed, the bisecting GlcNAc is lodged against the GlcNAcβ1–2 and Manα1–3 residues.

Interpretation of the Results. By use of the above linkage angles for the bisected structure, the NOE's were calculated (Table II) and found to be consistent with all the observed enhancements. The minimum energy conformer also predicted that NOE's should be observable between bis GN H4 and 3GN2 H5. This predicted NOE offered a plausible explanation for the additional NOE observed at 3.49 ppm in the NOE pattern obtained upon saturation of bis GN H4 (Figure 8d). As can be observed in Figure 8e on saturation on 3GN2 H1, the strongly coupled 3GN2 H4–H5 signal coincided with the enhanced signal at 3.49 ppm (in Figure 8d). Thus, bis GN H4 and 3GN2 H5 are within 3 Å of each other. The proximity of these two residues explains why the bis GN hydroxymethyl group is restricted to only one orientation (ω = −60°), since for ω = 180°, bis GN O6-H comes in too close contact with 3GN2 H5.

With the bis GN hydroxymethyl group fixed at ω = −60, an NOE between bis GN H6′ and 3i H2 is also expected. On saturation of 3i H2 the expected NOE for bis GN H6′ was too small to be detected (Figure 10c). However, since the chemical shift of the bis GN H6′ resonance was known (Figure 9a), it was irradiated, and an NOE was observed on 3i H2 (Figure 10b). Although the 3i H3 resonance is nearby, the NOE on 3i H2 did not arise from partial saturation of 3i H3, since when the irradiating frequency was moved 10 Hz downfield from the bis GN H6′ resonance position (i.e., closer to the frequency of the 3i H3 resonance), the NOE for 3i H2 was no longer observed (Figure 10d).

Since the bis GN is lodged against 3GN2 and 3i, perturbations on the chemical shifts of protons located in this interface are expected. Hence, differences in the ¹H chemical shifts for 3i and 3GN2 between GGN and GGN(GN) and between C3B and GNM₅ (Table I) are not due to alterations in conformation for the 3-arm. Usually, for a terminal

βGlcNAc residue, the H4 resonates near 3.5 ppm (i.e., 3GN2 in Table I). However, the bis GN H4 resonates near 3.26 ppm (Table I). The anomalous upfield shift of the bis GN H4 resonance could be due to the restricted orientation of the hydroxymethyl group for bis GN. For ω fixed at −60°, shielding contributions are expected to arise from the proximity of H6′ and from the proximity of 3GN2 H5 (Figure 6b), and in addition, the deshielding contribution, brought about by the proximity of O6 when ω = 180°, is no longer possible (Brisson & Carver, 1983a).

The orientation of the bis GN and the residues on the 3-arm should be similar in bisected complex and bisected hybrid structures, since on saturation of bis GN H4 in A3, a similar NOE pattern to that found for GGN(GN) was observed (Figure 4b). Although the chemical shifts for 3i, 3GN2, and bis GN in C3B and GGN(GN) are not the same (Table I), these differences are attributed to long-range effects brought about by the different structural units on the 6-arm (Brisson & Carver, 1983a).

Conclusion

In conclusion, no major conformational differences have been observed for the 3-arm of asparaginyl oligosaccharides drawn from five different structural classes. Furthermore, the three-dimensional structures deduced for the 3-arm of bisected structures lends a plausible explanation for its role in the biosynthetic pathway of asparaginyl oligosaccharides. Although this aspect will be discussed more fully elsewhere, it would appear that the highly inhibitory effect of the bisecting GlcNAc on at least four enzymes (Narasimhan, 1982) arises from the fact that this residue prevents access to a large surface of the 3-arm formed by the GlcNAcβ1–2Manα1–3Manβ1-unit. Thus, the probable mode of action of the bisecting GlcNAc in controlling the biosynthetic pathway of Asn-linked oligosaccharides is to prevent these enzymes from binding to their substrates.

References

Arnott, S., & Scott, W. E. (1972) *J. Chem. Soc., Perkin Trans. 2*, 324–335.

Biswas, M., & Rao, V. S. R. (1981) *Int. J. Quantum Chem. 20*, 99–121.

Brisson, J.-R., & Carver, J. P. (1982) *J. Biol. Chem. 257*, 11207–11209.

Brisson, J.-R., & Carver, J. P. (1983a) *Biochemistry* (following paper in this issue).

Brisson, J.-R., & Carver, J. P. (1983b) *Biochemistry 22*, 1362–1368.

Brisson, J.-R., & Carver, J. P. (1983c) *J. Biol. Chem. 258*, 1431–1434.

Carver, J. P., & Grey, A. A. (1981) *Biochemistry 20*, 6607–6616.

Carver, J. P., Grey, A. A., Winnik, F. M., Hakimi, J., Ceccarini, C., & Atkinson, P. H. (1981) *Biochemistry 20*, 6600–6606.

Cohen, R. E., & Ballou, C. E. (1980) *Biochemistry 19*, 4345-4358.

Cook, W. J., & Bugg, C. E. (1975) *Biochim. Biophys. Acta 389*, 428-435.

Dabrowski, J., Hanfland, P., & Egge, H. (1980) *Biochemistry 19*, 5652-5658.

Doddrell, D., Glushko, V., & Allerhand, A. (1972) *J. Chem. Phys. 56*, 3683-3689.

Dorland, L., Schut, B. L., Vliegenthart, J. F. G., Strecker, G., Fournet, B., Spik, G., & Montreuil, J. (1977) *Eur. J. Biochem. 73*, 93-97.

Fries, D. C., Rao, S. T., & Sundaral, M. (1971) *Acta Crystallogr., Sect. B B27*, 994-1005.

Goldstein, I. J., & Hayes, C. E. (1978) *Adv. Carbohydr. Chem. Biochem. 35*, 127-340.

Harpaz, N., & Schachter, H. (1980) *J. Biol. Chem. 255*, 4894-4902.

Hayes, M. L., Serianni, A. S., & Barker, R. (1982) *Carbohydr. Res. 100*, 87-101.

Hughes, R. C., & Sharon, N. (1978) *Nature (London) 274*, 637-638.

Jeffrey, G. A., McMullian, R. K., & Takagi, S. (1977) *Acta Crystallogr., Sect. B B33*, 728-737.

Lemieux, R. U., Bock, K., Delbaere, L. T. J., Koto, S., & Rao, V. S. (1980) *Can. J. Chem. 58*, 631-653.

Mo, F. (1979) *Acta Chem. Scand., Ser. A A33*, 207-218.

Narasimhan, S. (1982) *J. Biol. Chem. 257*, 10235-10242.

Noggle, J. H., & Schirmer, R. E. (1971) *The Nuclear Overhauser Effect*, Academic Press, New York.

Ogawa, T., & Yamamoto, H. (1982) *Carbohydr. Res. 104*, 271-283.

Potenzone, R., & Hopfinger, A. J. (1975) *Carbohydr. Res. 40*, 323-335.

Rees, D. A., & Skerett, R. J. (1970) *J. Chem. Soc. B*, 189-193.

Schachter, S., & Roseman, S. (1980) in *The Biochemistry of Glycoprotein and Proteoglycans* (Lennarz, W. J., Ed.) pp 85-160, Plenum Press, New York.

Sykes, B. D., Hull, W. E., & Snyder, G. H. (1978) *Biophys. J. 21*, 137-146.

Thogersen, H., Lemieux, R. U., Bock, K., & Meyer, B. (1982) *Can. J. Chem. 60*, 44-57.

Tvaroska, I., Perez, S., & Marchessault, R. H. (1978) *Carbohydr. Res. 61*, 97-106.

van Halbeek, H., Dorland, L., Veldink, G. A., Vliegenthart, J. F. G., Strecker, G., Michalski, J.-C., Montreuil, J., & Hull, W. E. (1980) *FEBS Lett. 121*, 71-77.

Warin, V., Baert, F., Fouret, R., Strecker, G., Spik, G., Fournet, B., & Montreuil, J. (1979) *Carbohydr. Res. 76*, 11-22.

Winnik, F. M., Brisson, J.-R., Carver, J. P., & Krepinsky, J. J. (1982a) *Carbohydr. Res. 103*, 15-28.

Winnik, F. M., Carver, J. P., & Krepinsky, J. J. (1982b) *J. Org. Chem. 47*, 2701-2707.

Solution Conformation of Asparagine-Linked Oligosaccharides: α(1-6)-Linked Moiety[†]

Jean-Robert Brisson and Jeremy P. Carver*

ABSTRACT: The solution conformation is presented for representatives of each of the major classes of asparaginyl oligosaccharides. In this report the conformation of the α(1-6)-linked moiety is described. The conformational properties of these glycopeptides were determined by high-resolution ^{1}H nuclear magnetic resonance in conjunction with potential energy calculations. The NMR parameters that were used in this analysis were chemical shifts and nuclear Overhauser enhancements. Potential energy calculations were used to evaluate the preferred conformers available for the different linkages in glycopeptides and to draw conclusions about the behavior in solution of these molecules. For all classes, identical conformations were found for the 6-arm *except* for the torsional angle, ω, about the C5-C6 bond of the α1-6 linkage. For high mannose and hybrid structures ω was found to be -60°, for bisected biantennary complex structures ω was 180°, and for complex biantennary structures averaging between -60° and 180° occurs.

In the preceding paper (Brisson & Carver, 1983a), the solution conformations of α(1-3)-, α(1-2)-, β(1-2)-, and β(1-4)-linked units of asparagine-linked oligosaccharides were examined. For all the major classes of glycopeptides, it was found that the conformation of any particular linkage was essentially the same from one to the other, although the conformations of different linkages were quite dissimilar. The inhibitory effect of the bisecting GlcNAc for certain enzymes involved in the biosynthetic pathway of glycopeptides (Narasimhan, 1982) was also explained. The position of the bisecting GlcNAc in the structure was found to be such that its ring covered a wide area on the surface of GlcNAcβ1-2Manα1-3Manβ1- unit, thus sterically hindering those enzymes from binding to this determinant.

In this paper the orientation of the α(1-6)-linked moiety in the different classes of N-linked oligosaccharides is described. In contrast to the invariance of the α1-3 linkage, major differences in the torsional angle about the C5-C6 bond of the α1-6 linkages are found.

Experimental Procedures

The experimental methods and methods of calculation are described in detail in the preceding paper (Brisson & Carver,